Context-dependent ATP7 Interactions with Parkinson's Disease-associated Genes Modulate Copper Homeostasis Phenotypes

Brooke M. Allen[1*], Nadia Gonzalez[2-3*], Erica Werner[4], Victor Faundez[4], and Alysia D. Vrailas-Mortimer[1-3, #]

1. Illinois State University, School of Biological Sciences, Normal, IL, USA
2. Oregon State University, Department of Biochemistry and Biophysics, Corvallis, OR, USA
3. Oregon State University, Linus Pauling Institute, Corvallis, OR, USA
4. Emory University, Department of Cell Biology, Atlanta, GA, USA

*Denotes equal contribution

Running Title: LRRK2 and Copper Homeostasis

Key words/phrases: LRRK2, ATP7, Copper Homeostasis, Parkinson's disease

Corresponding author:
Alysia D. Vrailas-Mortimer
Oregon State University
Department of Biochemistry and Biophysics
Corvallis, OR 97331
Phone: 541-737-9551
e-mail: Alysia.Mortimer@oregonstate.edu
ORCID: 0000-0001-5927-096X

Brooke Allen ORCID: 0009-0002-6028-3340
Nadia Gonzalez ORCID: 0009-0001-3889-6573
Erica Werner ORCID: 0000-0002-8183-16001
Victor Faundez ORCID: 0000-0002-2114-5271

Summary Statement

We performed a genetic interaction screen to explore the relationship between copper homeostasis and Parkinson's disease and other neurodegeneration associated genes.

Abstract

Copper is an essential micronutrient required by enzymes that catalyze oxygen-dependent reactions, but toxic in excess. Mutations in the ATP7A and ATP7B copper transporters cause neuropsychiatric symptoms and neurodegeneration by mechanisms that remain to be elucidated. We previously reported that the ATP7A biochemical interactome is enriched in Parkinson's disease (PD) and neurodegeneration associated proteins, yet the functional outcomes of these interactions are unknown. Using *Drosophila,* we tested genetic interactions between ATP7 mutants that alter copper levels and a subset of these PD and neurodegeneration causative genes and found sex differences with some candidate genes enhancing ATP7 deleterious phenotypes in both sexes, while others were sex specific. Most notably, we found that Lrrk2 (Lrrk), the most commonly mutated gene in familial forms of PD, protects against ATP7 dysfunction in epidermal epithelial cells with a stronger effect in males than females. However, in dopaminergic neurons Lrrk plays a role in intracellular copper induced toxicity in females but not males, supporting context dependent interactions between ATP7A and PD-associated genes to protect against disruptions in copper homeostasis.

Introduction

Copper is an essential micronutrient that acts as a structural component and catalytic cofactor for key cellular processes, such as antioxidant defense, mitochondrial respiration, energy and iron metabolism, and neurotransmitter production[1–3]. Disruptions in copper homeostasis can cause oxidative damage and impaired function of critical cuproenzymes, resulting in cellular dysfunction and cell death[4–6]. Therefore, copper homeostasis is tightly regulated within the cell by the copper transporters ATP7A and B which pump cytoplasmic copper into the lumen of the Golgi apparatus for metalation of secreted cuproenzymes. Excess levels of cytoplasmic copper, cause ATP7A/B translocation to the plasma membrane, pumping excess copper out of the cell[7–10]. Thus, deficiencies in ATP7B leads to copper accumulation at the cellular level and at the organism level, resulting in the neurodegenerative disorder Wilson's disease[5,6]. Whereas ATP7A mutations can cause Menkes disease, a multi-system disorder that includes widespread neurodegeneration caused by decreased copper in the brain due to defective dietary copper absorption[10,11]. Similarly, in the fruit fly, *Drosophila melanogaster*, genetic manipulation of the sole homologue *ATP7* causes a copper depletion phenotype affecting neuronal function[12] and structure[13] and induces early mortality[14]. We have found that ATP7A interacts with proteins associated with neurodegeneration and neurodevelopmental disorders[13], and ATP7A mutant

69 fibroblasts have altered expression of proteins associated with Parkinson's disease (PD) or
70 neurodegeneration, including elevated expression of the early onset neurodegenerative disease
71 protein, UCHL1[14]. Furthermore, we confirmed this link between ATP7 and UCHL1 through
72 genetic interactions in *Drosophila*[14].
73
74 PD is the second most common neurodegenerative disease and is characterized by loss
75 of dopaminergic neurons in the substantia nigra, impaired mitochondria, and increased oxidative
76 stress[15,16]. Familial forms of PD account for only 5-15% of cases, suggesting a strong
77 environmental component for this disease[15–17]. However, low brain copper levels can lead to
78 dysfunction and neurodegeneration as well, and copper levels are reduced in mice treated with
79 MPTP, a potent inducer of PD-like phenotypes[18,19]. Additionally, key mitochondrial proteins such
80 as Cytochrome c oxidase and superoxide dismutase (SOD1) are cuproenzymes, and ATP7A
81 mutant fibroblasts have impaired mitochondria[14,20]. Furthermore, both elevated and reduced
82 levels of copper can induce oxidative stress through different mechanisms[21,22], suggesting that
83 both increased and decreased levels of intracellular copper may contribute to PD. This is
84 supported by findings that administering $CuSO_4$ or Cu(II)(atsm) improve PD-like phenotypes in
85 mouse models[23–25], while other studies found improvement with treatment with a copper
86 chelator[26,27]. Furthermore, copper interacts with proteins mutated in familial forms of PD. DJ-1
87 can act as a copper chaperone to protect against metal toxicity[28,29], while copper binding to
88 alpha-synuclein promotes its aggregation[30,31]. In addition, loss of ATP7A exacerbated motor
89 phenotypes in a mouse alpha-synuclein (*SCNA*) model[32], and in *C. elegans*, PARKIN and
90 LRRK2 PD-like phenotypes were enhanced by environmental exposure to copper[33]. These data
91 suggest a strong connection between copper homeostasis and PD, however the mechanism
92 remains poorly understood.
93
94 To further explore this link between copper homeostasis and PD, we tested the
95 functional consequences of PD- or neurodegeneration associated genes that we identified as
96 ATP7A/B interactors in our previous proteomics screens[13,14] genetically interact with ATP7 using
97 the *Drosophila* model system, which we have shown recapitulates many of the phenotypes of
98 ATP7A/B human cell culture models[13,14,20,34]. We used two paradigms previously validated that
99 allow us to differentiate roles of copper homeostasis in non-neuronal cells (the epidermal
100 epithelium) and neuronal cells (dopaminergic neurons) in response to increased cellular copper
101 by ATP7 knockdown (RNAi) or copper depletion by overexpression of ATP7 in a cell
102 autonomous manner[13,20,34–37]. We find that inhibition of specific candidate genes enhances

ATP7 knockdown phenotypes in epidermal epithelial cells in a sex dependent manner with some genes showing interactions with both sexes while others only interacting in a sex-specific manner. We focused on Lrrk, the fly homologue of Lrrk2 which is the most commonly mutated gene in familial forms of PD and found that it genetically interacts with ATP7 in both males and females in the epidermal epithelium but only in female dopaminergic neurons. These data suggest that disruptions in copper homeostasis may broadly affect genes involved in PD/neurodegeneration and that these interactions may contribute to disease pathology.

Results

Coessentiality network analysis of ATP7A interactome

We previously found that loss of ATP7A, a model of increased cellular copper in human cells results in elevated levels of the neurodegeneration associated gene UCHL1 and that UCHL1 inhibition rescues ATP7 phenotypes in human cell culture and flies[38], suggesting that other neurodegeneration genes in the ATP7A interactome could modulate copper-dependent phenotypes as well. We first tested potential genetic interactions between ATP7A and the interactome PD/neurodegeneration genes by performing a coessentiality network analysis in silico (Figure S1). We assessed genome-scale fitness correlations between ATP7A with ARPC1A, ARPC1B, GIGYF2, HIP1, LRKK2, VPS13C and VPS35 mining the Dependency Map (DepMap) datasets[39,40]. Using the FIREWORKS tool (Fitness Interaction Rank-Extrapolated netWORKs)[41], we identified that correlated and anticorrelated genes reveal pathways and regulatory mechanisms connecting genes of interest with ATP7A positively (red edges) and negatively (blue edges) interacting with Parkinson's and neurodegeneration genes. These in silico findings support the model that ATP7A genetic interactions of similar complexity may also occur in mammals as we find in *Drosophila*.

ATP7 Genetically Interacts with Parkinson's Disease Genes

We next tested if these predicted interactions from our coessentiality network analysis are biological relevant using our fly ATP7 model (Table 1). In addition, we also tested two other interactome candidates SCYL1 (yata in flies), a neurodegeneration associated protein which had low expression levels, and the PD gene Synj1, which is a component of the endocytic pathway that was identified in the interactome (Table 1)[13,14]. Knockdown of ATP7 in the fly dorsal epidermal epithelium using pnr-GAL4 increases intracellular copper resulting in a decrease in pigmentation in a central stipe along the back of the fly in both females and males due to increased levels of intracellular copper (Figures 1B and 2B) as we and others have

137 previously observed. In addition, these flies also display a widening of the gap between the
138 midline bristles of the thorax (Figures 1B and 2B) as compared to out-crossed control pnr-GAL4
139 flies (Figures 1A and 2A). We next tested each of the ATP7A interactome genes and find that
140 knockdown of Arpc1 results in disorganized and missing midline bristles in females and males
141 (Figures S2B and S3B). Inhibition of either Gyf or yata results in missing scutellar bristles and
142 some loss of thoracic bristles (Figures S2C, J-L) in females with more mild phenotypes in males
143 (Figures S3C, J-L). Both Synj and Vps35 knockdown also leads to mild loss of scutellar bristles
144 in females and males (Figures S2E, I and S3E, I). We also observe sex differences with
145 inhibition of Hip1 and Vps13 which have no phenotype in females (Figures S2D, G-H) and mild
146 scutellar bristle loss in males (Figures S3D, G-H).
147
148 We next tested for genetic interactions between ATP7 down-regulation and inhibition of
149 these interactome genes. We find that in females, inhibition of either Arpc1, Hip1, or Vps13
150 enhances the ATP7 RNAi phenotype, resulting in a caved in thorax (Figure 1C, E, H, and Table
151 S1). In addition, the ATP7 RNAi phenotype is also enhanced in females with inhibition of yata
152 (line 1) with mild inhibition leading to increased bristle loss (Figure 1K and Table S1) and strong
153 inhibition (line 2) leading to lethality. We also observe an enhancement in disorganization of the
154 midline thoracic bristles when Vps35 was inhibited (Figure 1J and Table S1). However, not all of
155 the interactome genes interacted with ATP7 in females with neither inhibition of Gyf nor Synj
156 affecting the ATP7 down-regulation phenotype (Figure 1D, F-G and Table S1).
157
158 As ATP7 is on the X chromosome, males may be more sensitive to genetic perturbations
159 than females, and we find that similar to females Arpc1, Hip1, and Vps13 inhibition enhances
160 the ATP7 thorax caving in phenotype (Figure 2C, E, H and Table S1), though the effect of Arpc1
161 is not as strong as in females (Figure 2C vs 1C and Table S1). In addition, we find that mild
162 inhibition of yata (line 1) leads to a more severe enhancement of the ATP7 down-regulation
163 phenotype in males as compared to females (Figures 2K vs 1K and Table S1). Though Vps35
164 inhibition enhanced the ATP7 knockdown phenotype in females, we find no interaction in males
165 (Figure 2J and Table S1). In addition, unlike in females, inhibition of Synj (line 1) also leads to
166 enhancement of the phenotype (Figure 2F and Table S1), whereas similar to females Gyf
167 inhibition does not interact with ATP7 down-regulation in males (Figure 2D and Table S1).
168 These data suggest that normal expression of PD/neurodegeneration genes play a role in
169 protecting cells from increased intracellular copper and that males are more sensitive to these
170 perturbations.

171

172 *Inhibition of Lrrk enhances ATP7 down-regulation epidermal epithelium phenotypes*

173 Lrrk2 is the most commonly mutated gene in familial forms of PD[42] and regulates vesicular
174 trafficking, autophagy, and lysosomal function within cells[17,43–45]. Therefore, we next tested if the
175 Lrrk2 Drosophila orthologue, Lrrk, also plays a role in copper homeostasis using three different
176 RNAi lines (Table S2). We find that in both females and males, knockdown of Lrrk alone does
177 not affect the epidermal epithelium (Figures 3A-D, 4A-D, and Table S1). However, when
178 combined with down-regulation of ATP7, inhibition of Lrrk robustly enhanced the ATP7 RNAi
179 thorax phenotype, yet to a different extent across lines (Figures 3F-H, 4F-H, and Table S1).
180 Knockdown of Lrrk results in a more severe phenotype than in males than in females. For line 1,
181 some males present with necrosis of the scutellum (Figure 4F') and line 2 displayed a more
182 pronounced caving of the thorax (Figure 4G). In addition, we find that line 3 presented with mild
183 phenotypes in females (Figure 3H and Table S1), whereas males had a more pronounced
184 phenotype with increased thoracic caving (Figure 4H and Table S1) though these phenotypes
185 were milder than line 2 (Figure 4G and Table S1). These data suggest that Lrrk acts to protect
186 epidermal epithelial cells from high levels of intracellular copper and is a more potent interactor
187 in males.

188

189 *Lrrk and ATP7 down-regulation do not interact to regulate viability*

190 As inhibiting Lrrk leads to a worsening of the ATP7 down-regulation thorax phenotypes, we
191 tested if this alters organismal viability. Though down-regulation of ATP7 does not affect viability
192 in either females or males (Figure S4A, D and Table S3), Lrrk inhibition results in reduced
193 viability (Figure S4B-C, E-F and Table S3). Furthermore, inhibiting Lrrk in the ATP7 down-
194 regulation background reduces viability as compared to ATP7 knockdown alone, though this is
195 not significantly different from Lrrk inhibition alone (Figure S4B-C, E-F and Table S3). These
196 data show that the epithelial damage induced by disruption of the Lrrk and ATP7 interaction
197 spares animal viability.

198

199 *Inhibition of Lrrk rescues ATP7 down-regulation dopaminergic neuronal phenotypes in a sex*
200 *dependent manner*

201 We have previously found that altering copper homeostasis in dopaminergic neurons, which are
202 lost in PD, decreases survival to a copper challenge[13,14]. Therefore, we tested whether Lrrk
203 affects these outcomes. We find that in both females and males, inhibition of either ATP7 or Lrrk
204 alone or in combination does not affect survival on glucose only food (Table S4). Knockdown of

205 ATP7 decreases survival in females when exposed to copper, whereas knockdown of Lrrk did
206 not affect survival as compared to the GAL4 control line (Figure 5A-C, Table S5). However,
207 inhibiting Lrrk in the ATP7 knockdown background, rescued survival (Figure 5A-C, Table S5). In
208 contrast, males died faster when exposed to copper and had decreased survival when either
209 ATP7 or Lrrk is inhibited (Figure 5D-F, Table S5). Knocking down Lrrk in the ATP7 down-
210 regulation background did not significantly alter survival as compared to Lrrk or ATP7 down-
211 regulation (Figure 5D-F, Table S5). These data show that Lrrk contributes to the toxicity caused
212 by increased intracellular copper in females but not males.
213
214 *Inhibition of Lrrk enhances ATP7 over-expression epidermal epithelium phenotypes*
215 In humans, both increased intracellular copper and decreased intracellular copper lead to
216 neurological disorders, therefore, we tested if inhibition of Lrrk also interacts with decreased
217 copper levels modelled by over-expression of ATP7. As we and others have previously
218 reported, over-expression of ATP7 in the epidermal epithelium results in decreased
219 pigmentation and bristle loss in both males and females (Figures 3I and 4I and[9,20,34–38]). When
220 we combine inhibition of Lrrk with over-expression of ATP7, we find increased caving in of the
221 thorax (Figures 3J-L, 4J-L, and Table S1) and in some instances a darkening of the thorax
222 (Figure 3L and Figure 4K') that is indicative of underlying internal necrosis[46,47]. Therefore,
223 inhibition of Lrrk further enhances intracellular copper depletion thorax phenotypes in both
224 females and males. Taken together, our data suggest that Lrrk normally acts to protect against
225 both accumulation (Figures 3E-H, 4E-H, and Table S1) and depletion of intracellular copper
226 (Figures 3I-L, 4I-L, and Table S1).
227
228 *Inhibition of Lrrk reduces viability of ATP7 over-expression*
229 We next tested if Lrrk interacts with copper depletion for organismal viability and find that similar
230 to ATP7 down-regulation, over-expression of ATP7 does not affect viability (Figure 6 and Table
231 S6). However, inhibition of Lrrk in the ATP7 over-expression background reduces viability in
232 females and males (Figure 6B-C, E-F and Table S6) but only leads to a more severe reduction
233 as compared to Lrrk inhibition alone in females (Figure 6A-C and Table S6). These data indicate
234 that in females, Lrrk acts to protect epidermal epithelial cells from copper depletion but not
235 accumulation toxicity during development to promote survival to adulthood.
236
237 *Inhibition of Lrrk in dopaminergic neurons reduces survival of ATP7 over-expression in*
238 *response to environmental copper exposure*

239 As copper depletion in the brain leads to neurological disorders, we next tested if Lrrk interacts
240 with ATP7 over-expression in dopaminergic neurons. In females, over-expression of ATP7
241 leads to decreased survival, which is not affected by inhibition of Lrrk (Figure 7A-C, Table S7).
242 However, in males ATP7 over-expression had no effect on survival in response to copper
243 exposure though inhibition of Lrrk resulted in decreased survival (Figure 7D-F, Table S7). In
244 addition, Lrrk inhibition in the ATP7 over-expression background also led to decreased survival
245 to levels similar to Lrrk inhibition alone (Figure 7D-F, Table S7), suggesting that inhibition of Lrrk
246 does not sensitize the cell to copper depletion. Therefore, Lrrk does not interact with ATP7 over-
247 expression in dopaminergic neurons in response to environmental copper exposure.
248
249 **Discussion**
250 *Copper homeostasis and PD*
251 Copper dysregulation and PD share many key features including increased oxidative stress,
252 protein aggregation, and mitochondrial damage[21,22]. In addition, PD has been associated with
253 disruptions in copper homeostasis and copper-associated toxicity[21] with PD associated genes
254 intersecting with signaling pathways that regulate metal homeostasis and counteract oxidative
255 stress[44]. We have previously performed proteomic analyses to identify interactors of the copper
256 transporter ATP7A and identified a number of genes associated with PD and/or
257 neurodegeneration[13,14]. We further confirmed a genetic interaction between ATP7A and one of
258 these candidate genes, UCHL1, which is elevated in ATP7A mutant fibroblasts and inhibition of
259 UCHL1 rescued ATP7A phenotypes[14] and may be a potential target for the development of new
260 therapeutics. Here, we have further explored how wide-spread this relationship is by testing for
261 genetic interactions between ATP7 and other candidate genes from the ATP7A interactome[13,14].
262
263 We find that a subset (7 out of the 8 genes tested) genetically interact with ATP7 and
264 play a role in protecting epidermal epithelial cells from increased intracellular copper. Five of
265 these genes (Lrrk, Hip1, Synj, Vps13, and Vps35) are associated with PD, while Arpc1 (ARPC1)
266 interacts with known PD genes[48–51]. Two common themes emerge about the functions of those
267 genes that interacted with ATP7: 1) a role in mitochondrial function/health (Vps13, Vps35, and
268 Arpc1)[44,49,50,52–56] and 2) a role in endocytosis and Golgi trafficking (Vps13, Vps35, Arpc1, yata
269 and Hip1)[4,54,57–60]. In mammalian cell culture, VPS13C plays a role in ER-late
270 endosomes/lysosome communication[57] and localizes to the outer mitochondrial membrane[53]
271 where it may also mediate communication between the mitochondria and the ER/endosomal
272 system. Vps13 (VPS13C in mammals) also leads to mitochondrial dysfunction and damage and

273 plays a role in parkin/PINK1 mediated mitophagy[53]. Similarly, a mouse model of VPS35
274 recapitulated many PD phenotypes including mitochondrial dysfunction and damage[54] and
275 impaired mitophagy in SH-SY5Y cells[55]. Interestingly both VPS13C and VPS35 play a role in
276 iron homeostasis[61,62], along with our findings, these data suggest that these genes may play a
277 role in responding to metal dyshomeostasis. Arpc1 regulates actin polymerization and plays a
278 role in a variety of cellular processes including the endosomal trafficking[59]. Upon mitochondrial
279 damage, actin filaments are assembled by Arp2/3 around the damaged mitochondria and
280 inhibition of Arp2/3 impacts mitochondrial fusion[63] and parkin mediated mitophagy[56]. In addition
281 Arp2/3 is required for the function of the retromer complex, which includes VPS35[51], suggesting
282 that the nexus between mitochondrial and endosomal-lysosomal processes may be a key target
283 for the copper induced toxicity and PD.
284
285 Though HIP1 and yata have no known mitochondrial functions, they also play a role in
286 endocytosis and endosomal trafficking. HIP1 regulates clathrin-mediated endocytosis[60] and
287 trafficking of oxidative stress responsive cell receptors[64], and Hip1 loss of function has been
288 implicated in Huntington's disease, a neurodegenerative disorder in which oxidative stress and
289 mitochondrial dysfunction are prominent pathogenic features[65], suggesting that HIP1-dependent
290 trafficking may have downstream effects on mitochondrial homeostasis. yata (SCYL1 in
291 mammals) is associated with several neurodegenerative diseases and is an accessory factor for
292 the components of coatomer I (COPI) complex to regulate trafficking between the Golgi and
293 ER[58]. Inhibition of yata in both mice and flies leads to neurodegeneration[66,67] and interacts with
294 other proteins associated with neurodegenerative diseases such as APPL (Amyloid Precursor
295 Protein-like) in flies[66] and TDP-43 in mice[68]. We have previously found that ATP7 interacts with
296 the conserved oligomeric Golgi (COG) complex, a Golgi apparatus vesicular tether[20]. This
297 connection between intracellular trafficking and copper homeostasis suggests that when these
298 trafficking genes are disrupted it could exacerbate copper toxicity by impairing copper
299 sequestration, exocytosis, or recycling or metal binding proteins.
300
301 *Sex differences in response to copper dysregulation*
302 PD and other neurological disorders can present with skewed sex ratios. For example, men are
303 1.5 times more likely to develop PD than women[69,70]. In addition, as ATP7A is a sex-linked
304 gene, Menkes disease primarily affects males[71]. Similarly, we find sex-dependent interactions
305 among these genes with Synj interacting with ATP7 in males but not females. We also observed
306 differences in severity of phenotypes across sexes as Arpc1 has milder phenotypes in males

307 than females while yata and Lrrk have more severe phenotypes in males than in females. These
308 data suggest that males and females may have different protective mechanisms against copper
309 dysregulation that intersect with some PD-associated genes but not others.
310
311 *Lrrk and ATP7 interactions are context dependent*
312 Lrrk is a kinase that regulates diverse intracellular processes, such as: mitophagy, innate
313 immunity, vesicular transport, and autophagy[17,44,45], pathways that are frequently disrupted
314 during metal-induced stress, including copper toxicity[20,72–76].
315
316 We find that the interaction between Lrrk and ATP7 are dependent on the context. For example,
317 we find that Lrrk protects against both increased and depleted levels of intracellular copper in
318 epidermal epithelial cells to maintain thoracic structure in both sexes. However, in response to
319 increased copper, males are more severely affected when Lrrk is inhibited. Furthermore, only in
320 females and only during intracellular copper depletion in the epidermal epithelium does Lrrk act
321 to promote organismal viability. These interactions are also cell type specific as we find that
322 inhibition of Lrrk in females, but not males, improved survival in response to increased levels of
323 intracellular copper (ATP7 down-regulation with copper exposure) but had no effect on survival
324 in response to depletion of intracellular copper (ATP7 over-expression with copper exposure).
325 These data suggest that Lrrk contributes to intracellular copper toxicity, and since it plays a role
326 in stress response pathways[17], Lrrk2 may help buffer cells against copper-induced toxicity.
327 Additionally, as the pathogenic G2019S mutation in Lrrk is a gain of function mutation[77,78],
328 disruptions in copper homeostasis could lead to an earlier age of onset or more severe
329 symptoms/faster disease progression.
330
331 Through this study, we have confirmed that the ATP7A interactome identified from
332 human cell culture and patient samples[13,38], represent biologically significant interactions that
333 contribute to how cells respond to disruptions in cellular homeostasis. In addition, we also find
334 that there is an intimate and common connection between copper homeostasis and genetic
335 forms of PD, which may also provide new insights into how environmental exposure to copper
336 and other heavy metals contribute to sporadic forms of PD.
337
338 **Materials and Methods**
339 *Coessentiality Analysis*

340 Coessentiality Analysis was performed with the FIREWORKS engine[41] using ATP7A with
341 ARPC1A, ARPC1B, GIGYF2, HIP1, LRKK2, VPS13C and VPS35 genes as entries in the Pan-
342 Cancer dataset as Context. The engine was run with the top 5 primary nodes and the top five
343 secondary nodes positively and negatively correlated.
344
345 *Drosophila Strains and Husbandry*
346 The following strains were obtained from the Bloomington *Drosophila* Stock Center,
347 Bloomington, IL: w1118 (#5905), Ddc-Gal4 (#7009), pnr-Gal4 (#3039), UAS-Lrrk-RNAi-1
348 (#32457), UAS-Lrrk-RNAi-2 (#39019), and UAS-Lrrk-RNAi-3 (#35249). The UAS-ATP7-RNAi
349 (#108159) stock was obtained from the Vienna *Drosophila* Resource Center. The UAS-ATP7-wt
350 (overexpression) was a gift from Richard Burke, Monash University, Australia. See Table S2 for
351 a full list of genotypes. All stocks were reared on standard Molasses Food (Genesee Scientific)
352 at 25°C in 12hr:12hr light:dark cycle.
353
354 *Imaging*
355 ATP7A interactome candidate genes were knocked down in epidermal epithelium cells in either
356 an ATP7 loss of function or overexpression background using the pnr-Gal4 driver. 1-week-old
357 flies were imaged using a LEICA S6D stereomicroscope with a Leica EC4 Digital Camera. Z-
358 stacks were then aligned and max projections generated using Zerene Stacker.
359
360 *Viability Assay*
361 Three biological replicates of 8-10 virgin females were crossed with 4-5 males for each
362 genotype. The flies were transferred into new vials every three days resulting in three technical
363 replicates for each cross. Once the offspring began eclosing, they were tracked for nine days,
364 accounting for the number of males and females for each expected genotype were recorded. All
365 crosses were reared on standard Molasses Food (Genesee Scientific) at 25°C in 12hr:12hr
366 light:dark cycle.
367
368 *Copper Toxicity Assay*
369 Copper feedings were performed on 1-week-old virgin females and males reared separately.
370 ATP7 was either knockdown or overexpressed alone or in combination with Lrrk knockdown in
371 the dopaminergic neurons using the Ddc-Gal4 driver. Flies were starved for 3 hours and
372 transferred to empty vials with Whatman glass microfiber filter discs saturated in either 1 mM
373 $CuSO_4$ + 5% glucose solution or 5% glucose solution. Survival was assayed for every 12-24

hours for five days. Experiments were performed with a minimum of 10 replicates per genotype per sex with ~10 flies per replicate at 25°C in 12hr:12hr light:dark cycle.

Statistical Analysis

The results of the copper toxicity assay were tested for statistical significance testing survival and proportion data. Survival data was tested using Kaplan-Meier survival analysis, log-rank tests, and pairwise comparisons to assess the significance between genotypes and survival time. Proportion data for copper survival and viability were tested by creating a generalized linear model and an analysis of deviance table was used to fit variance using chi-squared tests for significance, per-time contrasts were conducted with post emmeans testing with tukey adjustment. All statistical analyses were performed in R.

Acknowledgements

We would also like to acknowledge the Bloomington Drosophila Stock Center (NIH P40OD018537) and the Vienna Drosophila Resource Center for providing fly stocks used in this study. Funding for this project included start-up funds from Illinois State University and Oregon State University, and R15AR070505 to AVM, and 1RF1AG060285 to VF. EW is supported by NIH grant ES034796 and NG is supported by 1T32GM160704-01. The content is solely the responsibility of the authors and does not necessarily represent the official views of the National Institutes of Health. The funders had no role in study design, data collection and analysis, decision to publish, or preparation of the manuscript.

Author Contributions

BA and NG performed experiments and data analysis. EW, VF, and AVM made intellectual contributions to experimental design, data analysis and interpretation, and provided funding. All authors were involved in reading and editing the manuscript.

Conflict of Interest Statement

The authors have no conflicts of interest.

Data Availability Statement

The data that support the findings of this study are available from the corresponding author upon reasonable request.

References

1. Henriksen, C., and Arnesen, E.K. (2023). Copper – a scoping review for Nordic Nutrition Recommendations 2023. Food Nutr. Res. *67*, 10.29219/fnr.v67.10322. https://doi.org/10.29219/fnr.v67.10322.

2. An, Y., Li, S., Huang, X., Chen, X., Shan, H., and Zhang, M. (2022). The Role of Copper Homeostasis in Brain Disease. Int. J. Mol. Sci. *23*, 13850. https://doi.org/10.3390/ijms232213850.

3. EFSA Panel on Dietetic Products, Nutrition and Allergies (NDA) (2015). Scientific Opinion on Dietary Reference Values for copper. EFSA J. *13*, 4253. https://doi.org/10.2903/j.efsa.2015.4253.

4. Lutsenko, S., Bhattacharjee, A., and Hubbard, A.L. (2010). Copper handling machinery of the brain. Met. Integr. Biometal Sci. *2*, 596–608. https://doi.org/10.1039/c0mt00006j.

5. Lutsenko, S., Barnes, N.L., Bartee, M.Y., and Dmitriev, O.Y. (2007). Function and Regulation of Human Copper-Transporting ATPases. Physiol. Rev. *87*, 1011–1046. https://doi.org/10.1152/physrev.00004.2006.

6. Chen, L., Min, J., and Wang, F. (2022). Copper homeostasis and cuproptosis in health and disease. Signal Transduct. Target. Ther. *7*, 378. https://doi.org/10.1038/s41392-022-01229-y.

7. Lane, A.R., Roberts, B.R., Fahrni, C.J., and Faundez, V. (2025). A primer on copper biology in the brain. Neurobiol. Dis. *212*, 106974. https://doi.org/10.1016/j.nbd.2025.106974.

8. Zlatic, S., Comstra, H.S., Gokhale, A., Petris, M.J., and Faundez, V. (2015). Molecular Basis of Neurodegeneration and Neurodevelopmental Defects in Menkes Disease. Neurobiol. Dis. *81*, 154–161. https://doi.org/10.1016/j.nbd.2014.12.024.

9. Hartwig, C., Zlatic, S.A., Wallin, M., Vrailas-Mortimer, A., Fahrni, C.J., and Faundez, V. (2019). Trafficking mechanisms of P-type ATPase copper transporters. Curr. Opin. Cell Biol. *59*, 24–33. https://doi.org/10.1016/j.ceb.2019.02.009.

10. Kaler, S.G. (2011). ATP7A-related copper transport diseases—emerging concepts and future trends. Nat. Rev. Neurol. *7*, 15–29. https://doi.org/10.1038/nrneurol.2010.180.

11. Tümer, Z., and Møller, L.B. (2010). Menkes disease. Eur. J. Hum. Genet. *18*, 511–518. https://doi.org/10.1038/ejhg.2009.187.

12. Hwang, J.E.C., de Bruyne, M., Warr, C.G., and Burke, R. (2014). Copper overload and deficiency both adversely affect the central nervous system of Drosophila. Met. Integr. Biometal Sci. *6*, 2223–2229. https://doi.org/10.1039/c4mt00140k.

13. Comstra, H.S., McArthy, J., Rudin-Rush, S., Hartwig, C., Gokhale, A., Zlatic, S.A., Blackburn, J.B., Werner, E., Petris, M., D'Souza, P., et al. (2017). The interactome of the copper transporter ATP7A belongs to a network of neurodevelopmental and neurodegeneration factors. eLife *6*, e24722. https://doi.org/10.7554/eLife.24722.

14. Zlatic, S.A., Vrailas-Mortimer, A., Gokhale, A., Carey, L.J., Scott, E., Burch, R., McCall, M.M., Rudin-Rush, S., Davis, J.B., Hartwig, C., et al. (2018). Rare Disease Mechanisms Identified by Genealogical Proteomics of Copper Homeostasis Mutant Pedigrees. Cell Syst. *6*, 368-380.e6. https://doi.org/10.1016/j.cels.2018.01.008.

15. Tysnes, O.-B., and Storstein, A. (2017). Epidemiology of Parkinson's disease. J. Neural Transm. *124*, 901–905. https://doi.org/10.1007/s00702-017-1686-y.

16. Pringsheim, T., Jette, N., Frolkis, A., and Steeves, T.D.L. (2014). The prevalence of Parkinson's disease: A systematic review and meta-analysis. Mov. Disord. *29*, 1583–1590. https://doi.org/10.1002/mds.25945.

17. Klein, C., and Westenberger, A. (2012). Genetics of Parkinson's Disease. Cold Spring Harb. Perspect. Med. *2*, a008888. https://doi.org/10.1101/cshperspect.a008888.

18. Alvarez-Vega, R., Rios, C., Rojas, P., and Kravsov, J. (1992). MPTP treatment decreases striatal copper content in mice. Proc. West. Pharmacol. Soc. *35*, 25–27.

19. Matusch, A., Depboylu, C., Palm, C., Wu, B., Höglinger, G.U., Schäfer, M.K.-H., and Becker, J.S. (2010). Cerebral bioimaging of Cu, Fe, Zn, and Mn in the MPTP mouse model of Parkinson's disease using laser ablation inductively coupled plasma mass spectrometry (LA-ICP-MS). J. Am. Soc. Mass Spectrom. *21*, 161–171. https://doi.org/10.1016/j.jasms.2009.09.022.

20. Hartwig, C., Méndez, G.M., Bhattacharjee, S., Vrailas-Mortimer, A.D., Zlatic, S.A., Freeman, A.A.H., Gokhale, A., Concilli, M., Werner, E., Sapp Savas, C., et al. (2021). Golgi-Dependent Copper Homeostasis Sustains Synaptic Development and Mitochondrial Content. J. Neurosci. Off. J. Soc. Neurosci. *41*, 215–233. https://doi.org/10.1523/JNEUROSCI.1284-20.2020.

21. Bisaglia, M., and Bubacco, L. (2020). Copper Ions and Parkinson's Disease: Why Is Homeostasis So Relevant? Biomolecules *10*, 195. https://doi.org/10.3390/biom10020195.

22. Davies, K.M., Bohic, S., Carmona, A., Ortega, R., Cottam, V., Hare, D.J., Finberg, J.P.M., Reyes, S., Halliday, G.M., Mercer, J.F.B., et al. (2014). Copper pathology in vulnerable brain regions in Parkinson's disease. Neurobiol. Aging *35*, 858–866. https://doi.org/10.1016/j.neurobiolaging.2013.09.034.

23. Hung, L.W., Villemagne, V.L., Cheng, L., Sherratt, N.A., Ayton, S., White, A.R., Crouch, P.J., Lim, S., Leong, S.L., Wilkins, S., et al. (2012). The hypoxia imaging agent CuII(atsm) is neuroprotective and improves motor and cognitive functions in multiple animal models of Parkinson's disease. J. Exp. Med. *209*, 837–854. https://doi.org/10.1084/jem.20112285.

24. Cheng, Y., Wang, G., Yang, X., Wang, Y., Li, D., Zhao, Y., and Zhang, F. (2025). Artesunate alleviates Parkinson's disease by targeting astrocyte MT2A to attenuate dopamine neuronal cuproptosis. Pharmacol. Res. *219*, 107895. https://doi.org/10.1016/j.phrs.2025.107895.

25. Alcaraz-Zubeldia, M., Rojas, P., Boll, C., and Ríos, C. (2001). Neuroprotective Effect of Acute and Chronic Administration of Copper (II) Sulfate against MPP+ Neurotoxicity in Mice. Neurochem. Res. *26*, 59–64. https://doi.org/10.1023/A:1007680616056.

26. Aguirre, P., García-Beltrán, O., Tapia, V., Muñoz, Y., Cassels, B.K., and Núñez, M.T. (2017). Neuroprotective Effect of a New 7,8-Dihydroxycoumarin-Based Fe2+/Cu2+ Chelator in Cell and Animal Models of Parkinson's Disease. ACS Chem. Neurosci. *8*, 178–185. https://doi.org/10.1021/acschemneuro.6b00309.

27. Leuci, R., Brunetti, L., Tufarelli, V., Cerini, M., Paparella, M., Puvača, N., and Piemontese, L. (2024). Role of copper chelating agents: between old applications and new perspectives in neuroscience. Neural Regen. Res. *20*, 751–762. https://doi.org/10.4103/NRR.NRR-D-24-00140.

28. Björkblom, B., Adilbayeva, A., Maple-Grødem, J., Piston, D., Ökvist, M., Xu, X.M., Brede, C., Larsen, J.P., and Møller, S.G. (2013). Parkinson disease protein DJ-1 binds metals and protects against metal-induced cytotoxicity. J. Biol. Chem. *288*, 22809–22820. https://doi.org/10.1074/jbc.M113.482091.

29. Girotto, S., Cendron, L., Bisaglia, M., Tessari, I., Mammi, S., Zanotti, G., and Bubacco, L. (2014). DJ-1 is a copper chaperone acting on SOD1 activation. J. Biol. Chem. *289*, 10887–10899. https://doi.org/10.1074/jbc.M113.535112.

30. Paik, S.R., Shin, H.J., and Lee, J.H. (2000). Metal-catalyzed oxidation of alpha-synuclein in the presence of Copper(II) and hydrogen peroxide. Arch. Biochem. Biophys. *378*, 269–277. https://doi.org/10.1006/abbi.2000.1822.

31. Walke, G., Kumar, R., and Wittung-Stafshede, P. (2024). Copper ion incorporation in α-synuclein amyloids. Protein Sci. Publ. Protein Soc. *33*, e4956. https://doi.org/10.1002/pro.4956.

32. Casey, M., Zou, D., Reijo Pera, R.A., Hensley-McBain, T., and Cabin, D.E. (2025). Alpha-synuclein null mutation exacerbates the phenotype of a model of Menkes disease in female mice. Front. Neurosci. *19*, 1613171. https://doi.org/10.3389/fnins.2025.1613171.

33. Weishaupt, A.-K., Ruecker, L., Meiners, T., Schwerdtle, T., Silva Avila, D., Aschner, M., and Bornhorst, J. (2024). Copper-mediated neurotoxicity and genetic vulnerability in the background of neurodegenerative diseases in C. elegans. Toxicol. Sci. Off. J. Soc. Toxicol. *201*, 254–262. https://doi.org/10.1093/toxsci/kfae092.

34. Lane, A.R., Scher, N.E., Bhattacharjee, S., Zlatic, S.A., Roberts, A.M., Gokhale, A., Singleton, K.S., Duong, D.M., McKenna, M., Liu, W.L., et al. (2025). Adaptive protein synthesis in genetic models of copper deficiency and childhood neurodegeneration. Mol. Biol. Cell *36*, ar33. https://doi.org/10.1091/mbc.E24-11-0512.

35. Hwang, J.E.C., de Bruyne, M., Warr, C.G., and Burke, R. (2014). Copper overload and deficiency both adversely affect the central nervous system of Drosophila†. Metallomics *6*, 2223–2229. https://doi.org/10.1039/c4mt00140k.

36. Norgate, M., Lee, E., Southon, A., Farlow, A., Batterham, P., Camakaris, J., and Burke, R. (2006). Essential roles in development and pigmentation for the Drosophila copper transporter DmATP7. Mol. Biol. Cell *17*, 475–484. https://doi.org/10.1091/mbc.e05-06-0492.

523 37. Burke, R., Commons, E., and Camakaris, J. (2008). Expression and localisation of the
524 essential copper transporter DmATP7 in Drosophila neuronal and intestinal tissues. Int. J.
525 Biochem. Cell Biol. *40*, 1850–1860. https://doi.org/10.1016/j.biocel.2008.01.021.

526 38. Zlatic, S.A., Vrailas-Mortimer, A., Gokhale, A., Carey, L.J., Scott, E., Burch, R., McCall,
527 M.M., Rudin-Rush, S., Davis, J.B., Hartwig, C., et al. (2018). Rare Disease Mechanisms
528 Identified by Genealogical Proteomics of Copper Homeostasis Mutant Pedigrees. Cell Syst.
529 *6*, 368-380.e6. https://doi.org/10.1016/j.cels.2018.01.008.

530 39. Arafeh, R., Shibue, T., Dempster, J.M., Hahn, W.C., and Vazquez, F. (2025). The present
531 and future of the Cancer Dependency Map. Nat. Rev. Cancer *25*, 59–73.
532 https://doi.org/10.1038/s41568-024-00763-x.

533 40. Tsherniak, A., Vazquez, F., Montgomery, P.G., Weir, B.A., Kryukov, G., Cowley, G.S., Gill,
534 S., Harrington, W.F., Pantel, S., Krill-Burger, J.M., et al. (2017). Defining a Cancer
535 Dependency Map. Cell *170*, 564-576.e16. https://doi.org/10.1016/j.cell.2017.06.010.

536 41. Amici, D.R., Jackson, J.M., Truica, M.I., Smith, R.S., Abdulkadir, S.A., and Mendillo, M.L.
537 (2021). FIREWORKS: a bottom-up approach to integrative coessentiality network analysis.
538 Life Sci. Alliance *4*. https://doi.org/10.26508/lsa.202000882.

539 42. Ravinther, A.I., Dewadas, H.D., Tong, S.R., Foo, C.N., Lin, Y.-E., Chien, C.-T., and Lim,
540 Y.M. (2022). Molecular Pathways Involved in LRRK2-Linked Parkinson's Disease: A
541 Systematic Review. Int. J. Mol. Sci. *23*, 11744. https://doi.org/10.3390/ijms231911744.

542 43. Taymans, J.-M., Fell, M., Greenamyre, T., Hirst, W.D., Mamais, A., Padmanabhan, S.,
543 Peter, I., Rideout, H., and Thaler, A. (2023). Perspective on the current state of the LRRK2
544 field. Npj Park. Dis. *9*, 104. https://doi.org/10.1038/s41531-023-00544-7.

545 44. Trinh, J., and Farrer, M. (2013). Advances in the genetics of Parkinson disease. Nat. Rev.
546 Neurol. *9*, 445–454. https://doi.org/10.1038/nrneurol.2013.132.

547 45. Sanna, G., Del Giudice, M.G., Crosio, C., and Iaccarino, C. (2012). LRRK2 and vesicle
548 trafficking. Biochem. Soc. Trans. *40*, 1117–1122. https://doi.org/10.1042/BST20120117.

549 46. Zhang, B., Binks, T., and Burke, R. (2020). The E3 ubiquitin ligase Slimb/β-TrCP is required
550 for normal copper homeostasis in *Drosophila*. Biochim. Biophys. Acta BBA - Mol. Cell Res.
551 *1867*, 118768. https://doi.org/10.1016/j.bbamcr.2020.118768.

552 47. Green, C., Levashina, E., McKimmie, C., Dafforn, T., Reichhart, J.M., and Gubb, D. (2000).
553 The necrotic gene in Drosophila corresponds to one of a cluster of three serpin transcripts
554 mapping at 43A1.2. Genetics *156*, 1117–1127. https://doi.org/10.1093/genetics/156.3.1117.

555 48. Karpenko, M.N., Muruzheva, Z.M., Ilyechova, E.Y., Babich, P.S., and Puchkova, L.V.
556 (2023). Abnormalities in Copper Status Associated with an Elevated Risk of Parkinson's
557 Phenotype Development. Antioxid. Basel Switz. *12*, 1654.
558 https://doi.org/10.3390/antiox12091654.

559 49. Kinnart, I., Manders, L., Heyninck, T., Imberechts, D., Praschberger, R., Schoovaerts, N.,
560 Verfaillie, C., Verstreken, P., and Vandenberghe, W. (2024). Elevated α-synuclein levels
561 inhibit mitophagic flux. NPJ Park. Dis. *10*, 80. https://doi.org/10.1038/s41531-024-00696-0.

562 50. Sarkar, S., Olsen, A.L., Sygnecka, K., Lohr, K.M., and Feany, M.B. (2021). α-synuclein
563 impairs autophagosome maturation through abnormal actin stabilization. PLoS Genet. *17*,
564 e1009359. https://doi.org/10.1371/journal.pgen.1009359.

565 51. Petyuk, V.A., Yu, L., Olson, H.M., Yu, F., Clair, G., Qian, W.-J., Shulman, J.M., and Bennett,
566 D.A. (2021). Proteomic Profiling of the Substantia Nigra to Identify Determinants of Lewy
567 Body Pathology and Dopaminergic Neuronal Loss. J. Proteome Res. *20*, 2266–2282.
568 https://doi.org/10.1021/acs.jproteome.0c00747.

569 52. Vidyadhara, D.J., Lee, J.E., and Chandra, S.S. (2019). Role of the Endolysosomal System
570 in Parkinson's disease. J. Neurochem. *150*, 487–506. https://doi.org/10.1111/jnc.14820.

571 53. Lesage, S., Drouet, V., Majounie, E., Deramecourt, V., Jacoupy, M., Nicolas, A., Cormier-
572 Dequaire, F., Hassoun, S.M., Pujol, C., Ciura, S., et al. (2016). Loss of VPS13C Function in
573 Autosomal-Recessive Parkinsonism Causes Mitochondrial Dysfunction and Increases
574 PINK1/Parkin-Dependent Mitophagy. Am. J. Hum. Genet. *98*, 500–513.
575 https://doi.org/10.1016/j.ajhg.2016.01.014.

576 54. Niu, M., Zhao, F., Bondelid, K., Siedlak, S.L., Torres, S., Fujioka, H., Wang, W., Liu, J., and
577 Zhu, X. (2021). VPS35 D620N knockin mice recapitulate cardinal features of Parkinson's
578 disease. Aging Cell *20*, e13347. https://doi.org/10.1111/acel.13347.

579 55. Ma, K.Y., Fokkens, M.R., Reggiori, F., Mari, M., and Verbeek, D.S. (2021). Parkinson's
580 disease-associated VPS35 mutant reduces mitochondrial membrane potential and impairs
581 PINK1/Parkin-mediated mitophagy. Transl. Neurodegener. *10*, 19.
582 https://doi.org/10.1186/s40035-021-00243-4.

583 56. Fung, T.S., Ghosh, A., Zavala, M.R., Nichtova, Z., Shukal, D., Tigano, M., Csordas, G.,
584 Higgs, H.N., and Chakrabarti, R. (2025). Peri-mitochondrial actin filaments inhibit Parkin
585 assembly by disrupting ER-mitochondria contacts. EMBO Rep., 1–32.
586 https://doi.org/10.1038/s44319-025-00561-y.

587 57. Kumar, N., Leonzino, M., Hancock-Cerutti, W., Horenkamp, F.A., Li, P., Lees, J.A., Wheeler,
588 H., Reinisch, K.M., and De Camilli, P. (2018). VPS13A and VPS13C are lipid transport
589 proteins differentially localized at ER contact sites. J. Cell Biol. *217*, 3625–3639.
590 https://doi.org/10.1083/jcb.201807019.

591 58. Burman, J.L., Bourbonniere, L., Philie, J., Stroh, T., Dejgaard, S.Y., Presley, J.F., and
592 McPherson, P.S. (2008). Scyl1, mutated in a recessive form of spinocerebellar
593 neurodegeneration, regulates COPI-mediated retrograde traffic. J. Biol. Chem. *283*, 22774–
594 22786. https://doi.org/10.1074/jbc.M801869200.

595 59. Taunton, J., Rowning, B.A., Coughlin, M.L., Wu, M., Moon, R.T., Mitchison, T.J., and
596 Larabell, C.A. (2000). Actin-dependent propulsion of endosomes and lysosomes by
597 recruitment of N-WASP. J. Cell Biol. *148*, 519–530. https://doi.org/10.1083/jcb.148.3.519.

598 60. Buenaventura, T., Kanda, N., Douzenis, P.C., Jones, B., Bloom, S.R., Chabosseau, P.,
599 Corrêa, I.R., Bosco, D., Piemonti, L., Marchetti, P., et al. (2018). A Targeted RNAi Screen
600 Identifies Endocytic Trafficking Factors That Control GLP-1 Receptor Signaling in
601 Pancreatic β-Cells. Diabetes *67*, 385–399. https://doi.org/10.2337/db17-0639.

602 61. Xue, Y., Schmollinger, S., Attar, N., Campos, O.A., Vogelauer, M., Carey, M.F., Merchant,
603 S.S., and Kurdistani, S.K. (2017). Endoplasmic reticulum-mitochondria junction is required
604 for iron homeostasis. J. Biol. Chem. *292*, 13197–13204.
605 https://doi.org/10.1074/jbc.M117.784249.

606 62. Bórquez, D.A., Castro, F., Núñez, M.T., and Urrutia, P.J. (2022). New Players in Neuronal
607 Iron Homeostasis: Insights from CRISPRi Studies. Antioxid. Basel Switz. *11*, 1807.
608 https://doi.org/10.3390/antiox11091807.

609 63. Gatti, P., Schiavon, C., Cicero, J., Manor, U., and Germain, M. (2025). Mitochondria- and
610 ER-associated actin are required for mitochondrial fusion. Nat. Commun. *16*, 451.
611 https://doi.org/10.1038/s41467-024-55758-x.

612 64. Metzler, M., Li, B., Gan, L., Georgiou, J., Gutekunst, C.-A., Wang, Y., Torre, E., Devon,
613 R.S., Oh, R., Legendre-Guillemin, V., et al. (2003). Disruption of the endocytic protein HIP1
614 results in neurological deficits and decreased AMPA receptor trafficking. EMBO J. *22*,
615 3254–3266. https://doi.org/10.1093/emboj/cdg334.

616 65. Bhattacharyya, N.P., Banerjee, M., and Majumder, P. (2008). Huntington's disease: roles of
617 huntingtin-interacting protein 1 (HIP-1) and its molecular partner HIPPI in the regulation of
618 apoptosis and transcription. FEBS J. *275*, 4271–4279. https://doi.org/10.1111/j.1742-
619 4658.2008.06563.x.

620 66. Sone, M., Uchida, A., Komatsu, A., Suzuki, E., Ibuki, I., Asada, M., Shiwaku, H., Tamura, T.,
621 Hoshino, M., Okazawa, H., et al. (2009). Loss of yata, a novel gene regulating the
622 subcellular localization of APPL, induces deterioration of neural tissues and lifespan
623 shortening. PloS One *4*, e4466. https://doi.org/10.1371/journal.pone.0004466.

624 67. Schmidt, W.M., Kraus, C., Höger, H., Hochmeister, S., Oberndorfer, F., Branka, M.,
625 Bingemann, S., Lassmann, H., Müller, M., Macedo-Souza, L.I., et al. (2007). Mutation in the
626 Scyl1 gene encoding amino-terminal kinase-like protein causes a recessive form of
627 spinocerebellar neurodegeneration. EMBO Rep. *8*, 691–697.
628 https://doi.org/10.1038/sj.embor.7401001.

629 68. Pelletier, S., Gingras, S., Howell, S., Vogel, P., and Ihle, J.N. (2012). An early onset
630 progressive motor neuron disorder in Scyl1-deficient mice is associated with mislocalization
631 of TDP-43. J. Neurosci. Off. J. Soc. Neurosci. *32*, 16560–16573.
632 https://doi.org/10.1523/JNEUROSCI.1787-12.2012.

633 69. Cerri, S., Mus, L., and Blandini, F. Parkinson's Disease in Women and Men: What's the
634 Difference? J. Park. Dis. *9*, 501–515. https://doi.org/10.3233/JPD-191683.

635 70. Moisan, F., Kab, S., Mohamed, F., Canonico, M., Guern, M.L., Quintin, C., Carcaillon, L.,
636 Nicolau, J., Duport, N., Singh-Manoux, A., et al. (2016). Parkinson disease male-to-female
637 ratios increase with age: French nationwide study and meta-analysis. J. Neurol. Neurosurg.
638 Psychiatry *87*, 952–957. https://doi.org/10.1136/jnnp-2015-312283.

639 71. Tümer, Z., and Møller, L.B. (2010). Menkes disease. Eur. J. Hum. Genet. *18*, 511–518.
640 https://doi.org/10.1038/ejhg.2009.187.

641 72. Aschner, M., Skalny, A.V., Lu, R., Martins, A.C., Tizabi, Y., Nekhoroshev, S.V., Santamaria,
642 A., Sinitskiy, A.I., and Tinkov, A.A. (2024). Mitochondrial pathways of copper neurotoxicity:
643 focus on mitochondrial dynamics and mitophagy. Front. Mol. Neurosci. *17*, 1504802.
644 https://doi.org/10.3389/fnmol.2024.1504802.

645 73. Lu, J., Liu, X., Li, X., Li, H., Shi, L., Xia, X., He, B.-L., Meyer, T.F., Li, X., Sun, H., et al.
646 (2024). Copper regulates the host innate immune response against bacterial infection via
647 activation of ALPK1 kinase. Proc. Natl. Acad. Sci. U. S. A. *121*, e2311630121.
648 https://doi.org/10.1073/pnas.2311630121.

649 74. O'Sullivan, E., O'Shea, D., Devereux, M., Kavanagh, K., and Howe, O. (2026). Autophagy-
650 dependent cell death and immune responses induced by heteroleptic copper(II),
651 manganese(II), and silver(I) complexes containing dicarboxylate and 1,10-phenanthroline
652 ligands: novel insights from in vitro and in vivo models. Biometals Int. J. Role Met. Ions Biol.
653 Biochem. Med. *39*, 337–358. https://doi.org/10.1007/s10534-025-00766-7.

654 75. Duncan, C., Bica, L., Crouch, P.J., Caragounis, A., Lidgerwood, G.E., Parker, S.J.,
655 Meyerowitz, J., Volitakis, I., Liddell, J.R., Raghupathi, R., et al. (2013). Copper modulates
656 the large dense core vesicle secretory pathway in PC12 cells. Met. Integr. Biometal Sci. *5*,
657 700–714. https://doi.org/10.1039/c3mt20231c.

658 76. Seo, Y., Cho, Y.-S., Huh, Y.-D., and Park, H. (2016). Copper Ion from Cu2O Crystal Induces
659 AMPK-Mediated Autophagy via Superoxide in Endothelial Cells. Mol. Cells *39*, 195–203.
660 https://doi.org/10.14348/molcells.2016.2198.

661 77. Lee, B.D., Shin, J.-H., VanKampen, J., Petrucelli, L., West, A.B., Ko, H.S., Lee, Y.-I.,
662 Maguire-Zeiss, K.A., Bowers, W.J., Federoff, H.J., et al. (2010). Inhibitors of leucine-rich
663 repeat kinase-2 protect against models of Parkinson's disease. Nat. Med. *16*, 998–1000.
664 https://doi.org/10.1038/nm.2199.

665 78. Liu, Z., Wang, X., Yu, Y., Li, X., Wang, T., Jiang, H., Ren, Q., Jiao, Y., Sawa, A., Moran, T.,
666 et al. (2008). A Drosophila model for LRRK2-linked parkinsonism. Proc. Natl. Acad. Sci. U.
667 S. A. *105*, 2693–2698. https://doi.org/10.1073/pnas.0708452105.

668

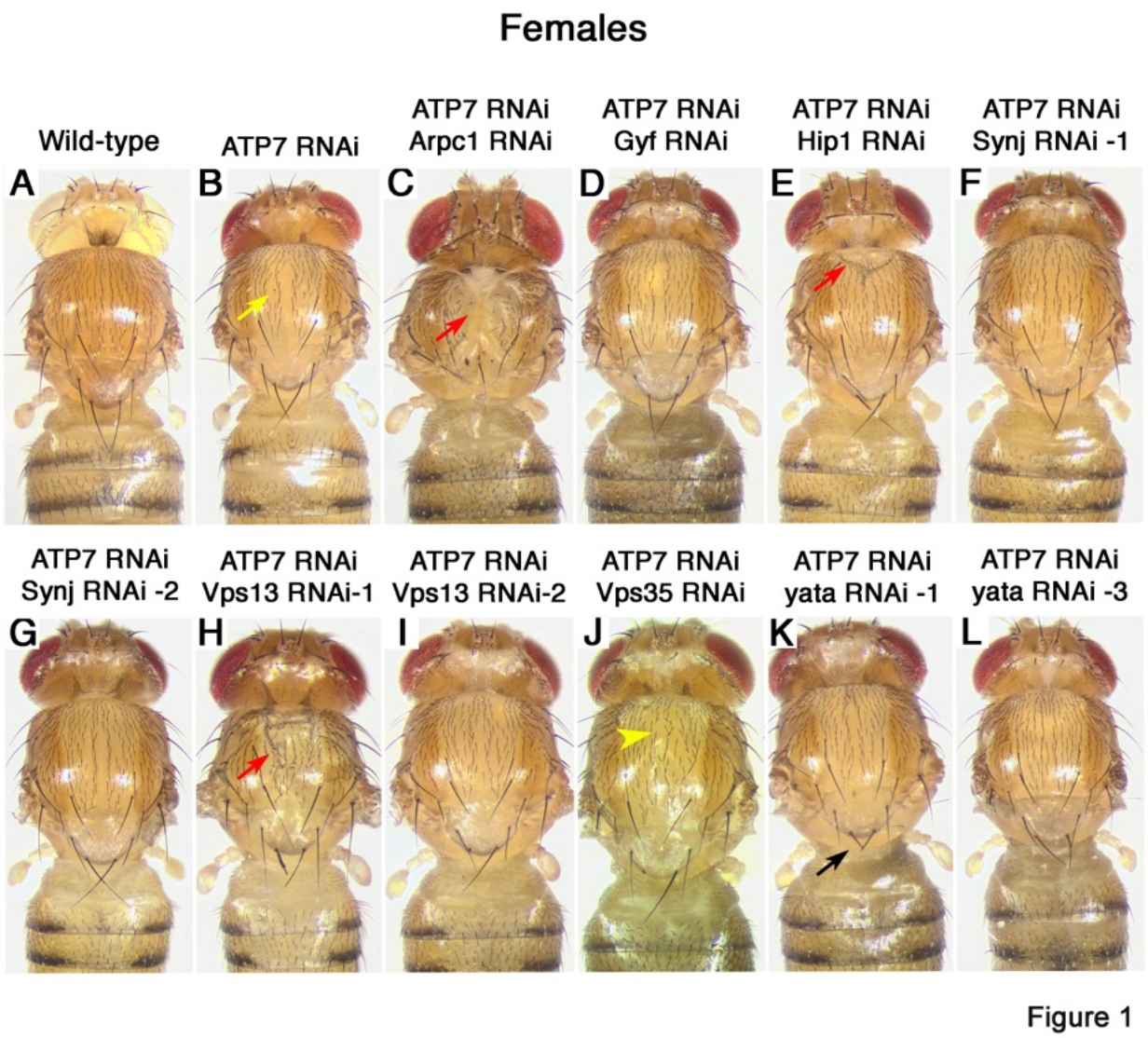

Figure 1. ATP7 Interacts with Parkinson's Disease/Neurodegeneration Genes in the Epidermal Epithelium in Females. Images of inhibition of ATP7 alone **A)** or in combination with inhibition of different ATP7 interactome homologues using the pnr-GAL4 in females **B-L).** Yellow arrows indicate widening of the thoracic midline bristles, red arrows indicate areas of thoracic caving in, black arrows show scutellar bristle defects, and yellow arrowhead indicates bristle disorganization.

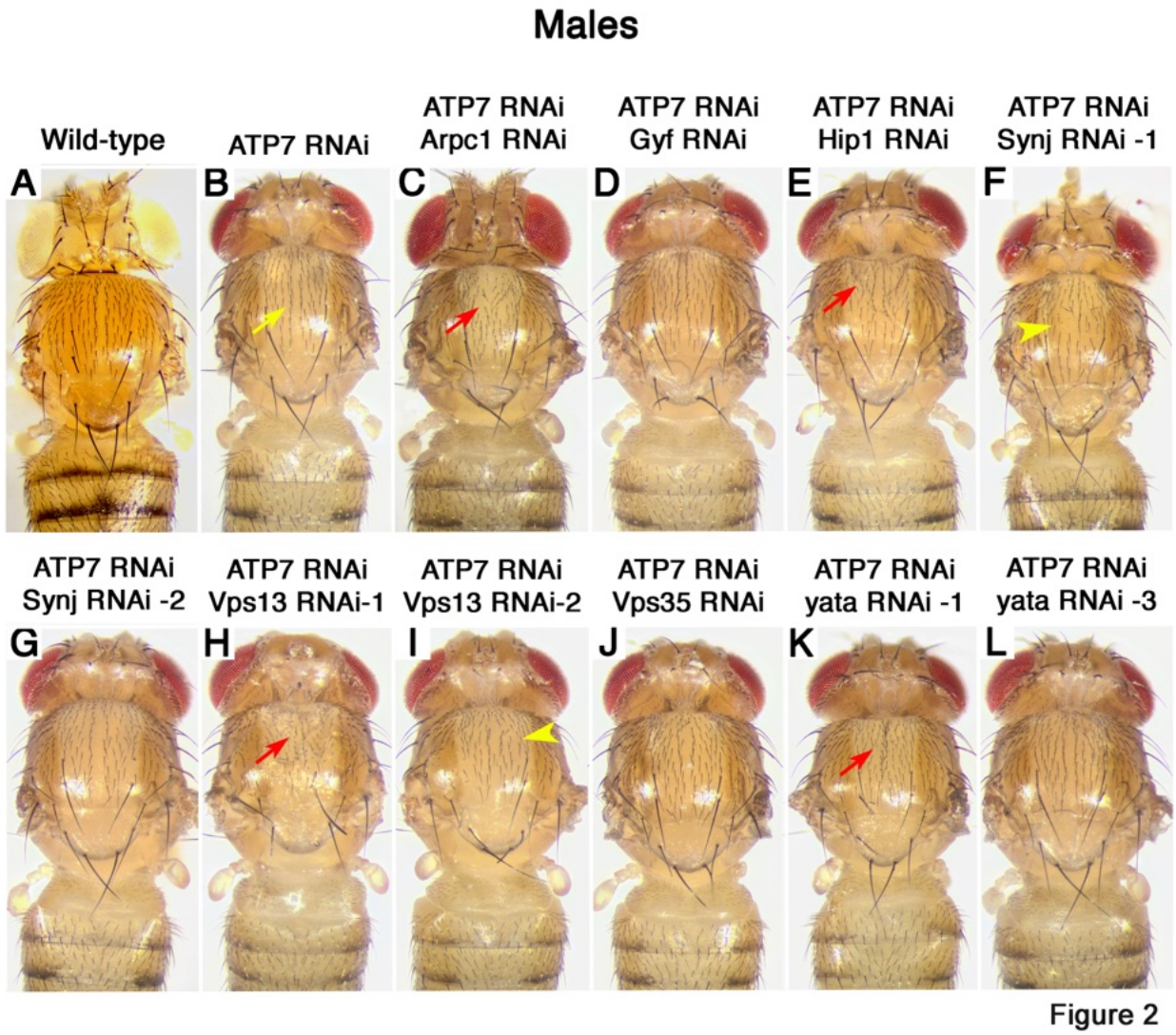

Figure 2. ATP7 Interacts with Parkinson's Disease/Neurodegeneration Genes in the Epidermal Epithelium in Males. Images of inhibition of ATP7 alone **A)** or in combination with inhibition of different ATP7 interactome homologues using the pnr-GAL4 in males **B-L).** Yellow arrows indicate areas of thoracic caving in, and red arrows indicate areas of thoracic caving in, black arrows show scutellar bristle defects, and yellow arrowhead indicates missing and disorganized thoracic bristles.

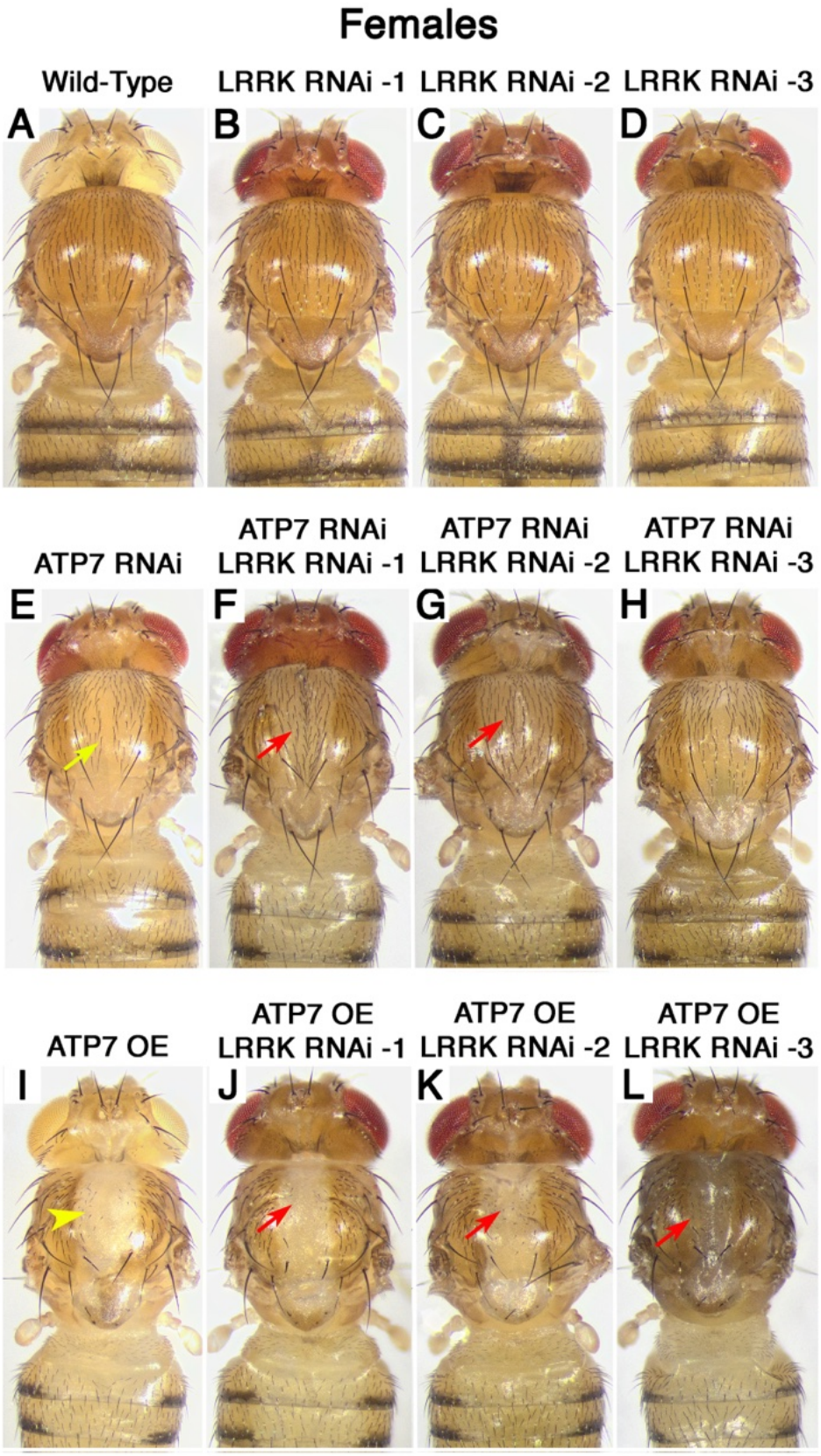
Females
Wild-Type
LRRK RNAi -1
LRRK RNAi -2
LRRK RNAi -3
A
B
C
D
ATP7 RNAi
ATP7 RNAi
LRRK RNAi -1
ATP7 RNAi
LRRK RNAi -2
ATP7 RNAi
LRRK RNAi -3
E
F
G
H
ATP7 OE
ATP7 OE
LRRK RNAi -1
ATP7 OE
LRRK RNAi -2
ATP7 OE
LRRK RNAi -3
I
J
K
L

Figure 3

Figure 3. ATP7 Interacts with Lrrk in the Epidermal Epithelium in Females. Images of control **A)** and different Lrrk RNAi lines **B-D)** using the pnr-GAL4 in females**.** ATP7 down-regulation alone **E)** or in combination with inhibition of Lrrk **F-H).** ATP7 over-expression **I)** alone or in combination with inhibition of Lrrk **J-L)**. Yellow arrows indicate widening of the bristles along the midline of the thorax. Red arrows indicate thoracic caving in, and yellow arrowheads indicate bristle loss.

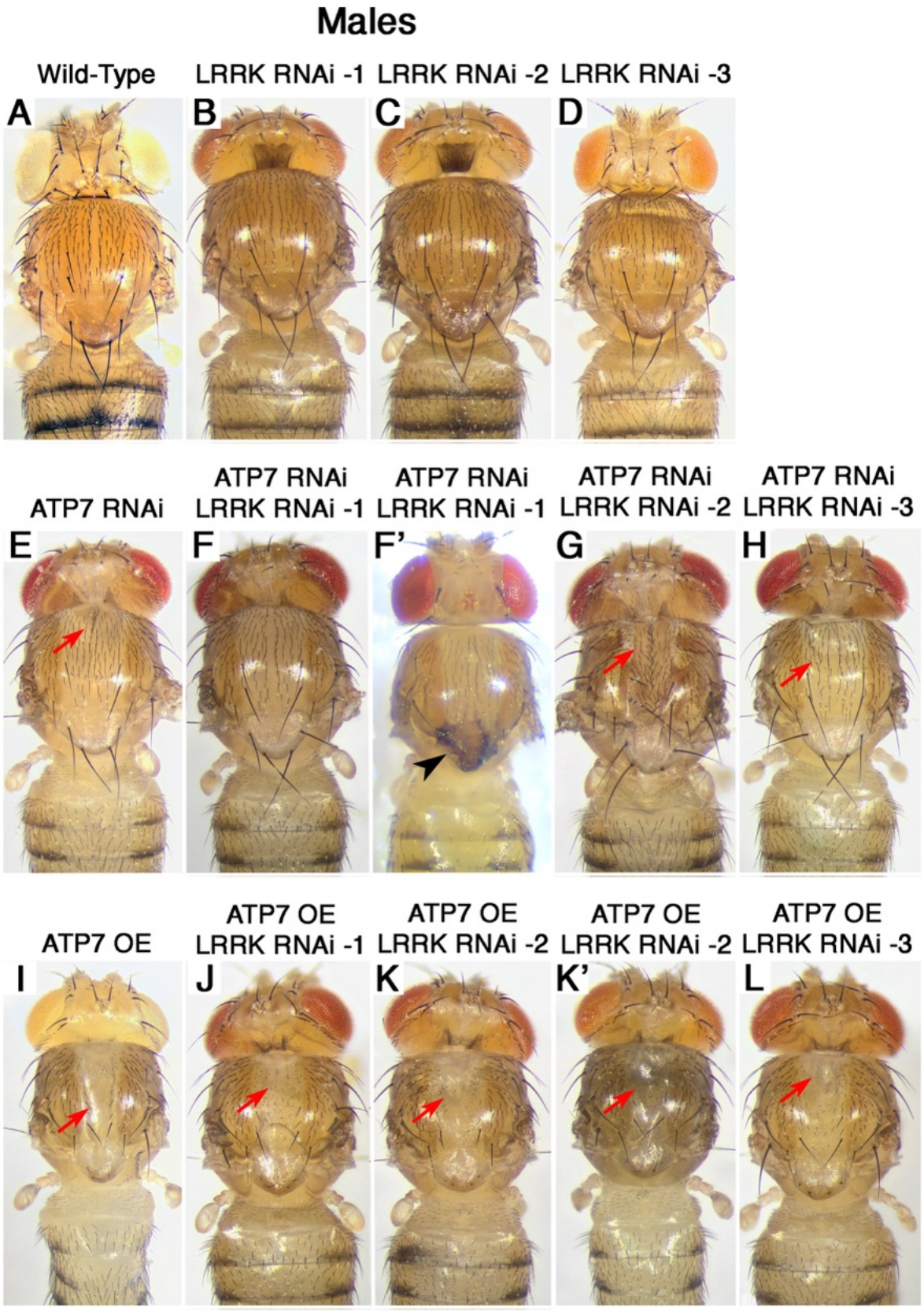
Males
Wild-Type
LRRK RNAi -1
LRRK RNAi -2
LRRK RNAi -3
A
B
C
D
ATP7 RNAi
ATP7 RNAi
LRRK RNAi -1
ATP7 RNAi
LRRK RNAi -1
ATP7 RNAi
LRRK RNAi -2
ATP7 RNAi
LRRK RNAi -3
E
F
F'
G
H
ATP7 OE
ATP7 OE
LRRK RNAi -1
ATP7 OE
LRRK RNAi -2
ATP7 OE
LRRK RNAi -2
ATP7 OE
LRRK RNAi -3
I
J
K
K'
L

Figure 4

Figure 4. ATP7 Interacts with Lrrk in the Epidermal Epithelium in Males. Images of control **A)** and different Lrrk RNAi lines **B-D)** using the pnr-GAL4 in males**.** ATP7 down-regulation alone **E)** or in combination with inhibition of Lrrk **F-H).** ATP7 over-expression **I)** alone or in combination with inhibition of Lrrk **J-L)**. Red arrows indicate thoracic caving in, and black arrowheads indicate necrotic tissue.

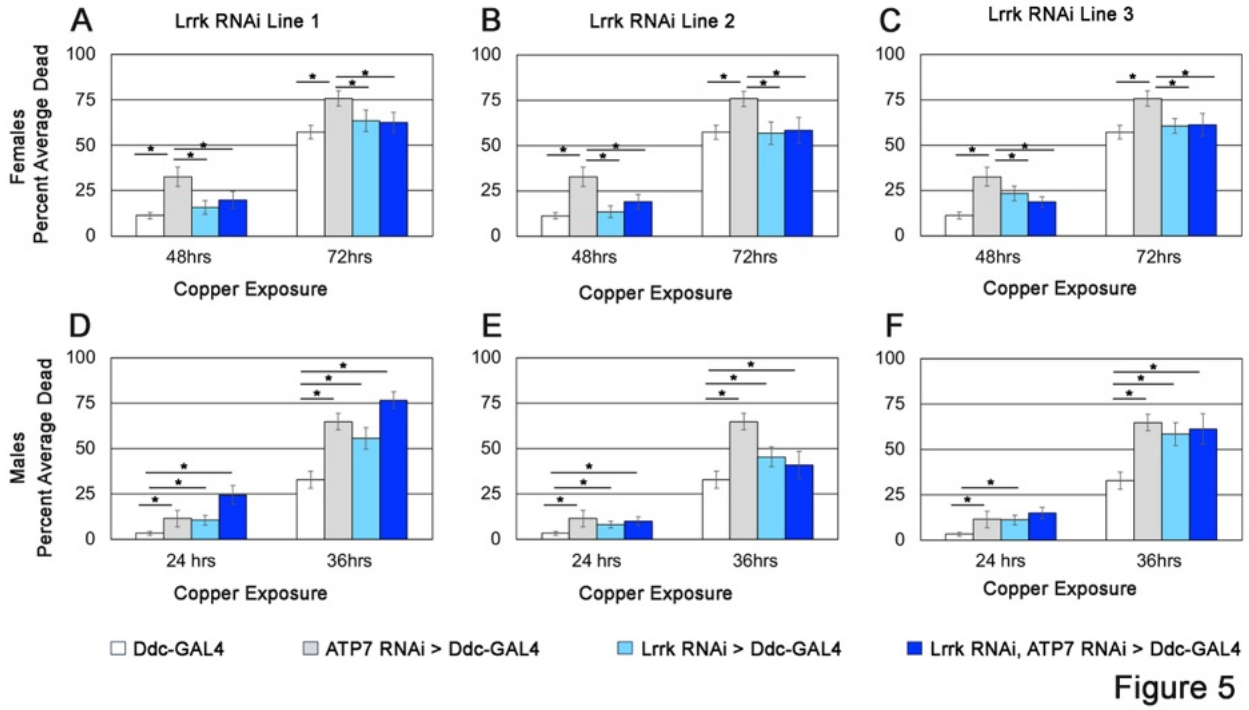

Figure 5. Lrrk Interacts with ATP7 Down-regulation and Copper Exposure in Dopaminergic Neurons. Female **A-C)** and male **D-F)** flies exposed to copper with either inhibition of ATP7 alone or in combination with Lrrk inhibition using the Ddc-GAL4.

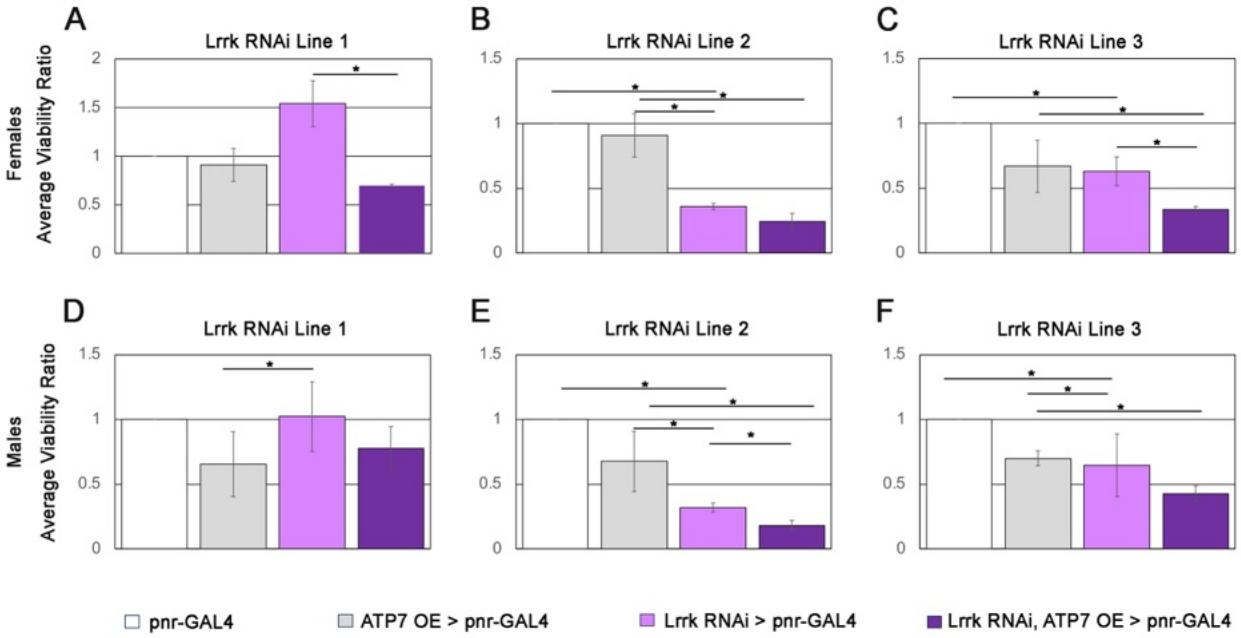

Figure 6. Lrrk Interacts with ATP7 Over-expression and Viability. The normalized ratio of female **A-C)** and male **D-F)** flies that were expected to reach adulthood (viability) with either down-regulation of ATP7 alone or in combination with Lrrk inhibition using the Ddc-GAL4. For Lrrk RNAi line 1 females, statistical results χ^2 = 10.93, df = 3, p-value = 0.01211. For Lrrk RNAi line 2 females, statistical results χ^2 = 120.44, df = 3, p-value < 2.2e-16. For Lrrk RNAi line 3 females, statistical results χ^2 = 41.642, df = 3, p-value = 4.778e-09. For Lrrk RNAi line 1 males, statistical results χ^2 = 12.034, df = 3, p-value = 0.007268. For Lrrk RNAi line 2 males, statistical results χ^2 = 141.32, df = 3, p-value < 2.2e-16. For Lrrk RNAi line 3 females, statistical results χ^2 = 31.117, df = 3, p-value = 8.03e-07.

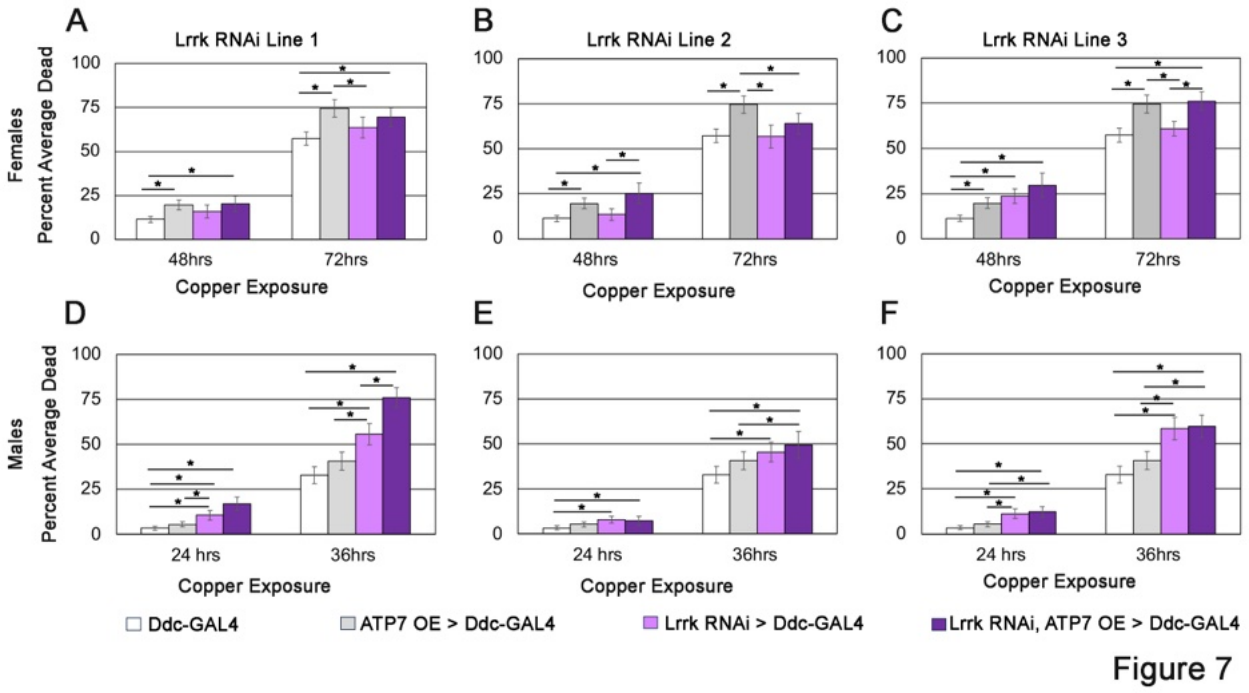

Figure 7. Lrrk Interacts with ATP7 Over-expression and Copper Exposure in Dopaminergic Neurons. Female **A-C)** and male **D-F)** flies exposed to copper with either over-expression of ATP7 alone or in combination with Lrrk inhibition using the Ddc-GAL4.

Drosophila Candidate Gene	Drosophila Gene Abbreviation	Human Homolog Gene Name	Human Homolog Abbreviation	OMIM Number	PARK Number
Actin-related protein 2/3 complex, subunit 1	Arpc1	Actin-Related Protein 2/3 Complex	ARPC1	604223	N/A
Gigyf	Gyf	GRB10 interaction GYF protein 2	GIGYF2	607688	N/A
Huntingtin interacting protein 1	Hip1	Huntingtin interacting protein 1	HIP1	601767	PARK11
Leucine-rich repeat kinase	Lrrk	Leucine rich repeat kinase 2	Lrrk2	607060	PARK8
Synaptojanin	Synj	Synaptojanin 1	Synj1	615530	PARK20
Vacuolar protein sorting 13	Vps13	Vacuolar protein sorting 13C	VPS13C	616840	PARK23
Vacuolar protein sorting 35	Vps35	VPS35 retromer complex component	VPS35	601501	PARK17
yata	yata	SCYL like pseudokinase 1	SCYL1	616719	N/A

Table 1. *Drosophila* Homologues of ATP7A Interactome Genes